Constitutive Modeling of Piezoelectric Polymer Composites

Gregory M. Odegard
National Institute of Aerospace, Hampton, Virginia

December 2003

The NASA STI Program Office . . . in Profile

Since its founding, NASA has been dedicated to the advancement of aeronautics and space science. The NASA Scientific and Technical Information (STI) Program Office plays a key part in helping NASA maintain this important role.

The NASA STI Program Office is operated by Langley Research Center, the lead center for NASA's scientific and technical information. The NASA STI Program Office provides access to the NASA STI Database, the largest collection of aeronautical and space science STI in the world. The Program Office is also NASA's institutional mechanism for disseminating the results of its research and development activities. These results are published by NASA in the NASA STI Report Series, which includes the following report types:

- TECHNICAL PUBLICATION. Reports of completed research or a major significant phase of research that present the results of NASA programs and include extensive data or theoretical analysis. Includes compilations of significant scientific and technical data and information deemed to be of continuing reference value. NASA counterpart of peer-reviewed formal professional papers, but having less stringent limitations on manuscript length and extent of graphic presentations.

- TECHNICAL MEMORANDUM. Scientific and technical findings that are preliminary or of specialized interest, e.g., quick release reports, working papers, and bibliographies that contain minimal annotation. Does not contain extensive analysis.

- CONTRACTOR REPORT. Scientific and technical findings by NASA-sponsored contractors and grantees.

- CONFERENCE PUBLICATION. Collected papers from scientific and technical conferences, symposia, seminars, or other meetings sponsored or co-sponsored by NASA.

- SPECIAL PUBLICATION. Scientific, technical, or historical information from NASA programs, projects, and missions, often concerned with subjects having substantial public interest.

- TECHNICAL TRANSLATION. English-language translations of foreign scientific and technical material pertinent to NASA's mission.

Specialized services that complement the STI Program Office's diverse offerings include creating custom thesauri, building customized databases, organizing and publishing research results . . . even providing videos.

For more information about the NASA STI Program Office, see the following:

- Access the NASA STI Program Home Page at *http://www.sti.nasa.gov*

- Email your question via the Internet to help@sti.nasa.gov

- Fax your question to the NASA STI Help Desk at (301) 621-0134

- Telephone the NASA STI Help Desk at (301) 621-0390

- Write to:
  NASA STI Help Desk
  NASA Center for AeroSpace Information
  7121 Standard Drive
  Hanover, MD 21076-1320

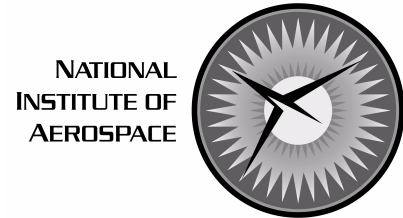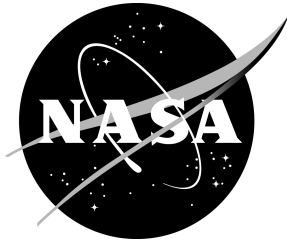# Constitutive Modeling of Piezoelectric Polymer Composites

Gregory M. Odegard
National Institute of Aerospace, Hampton, Virginia

CONSTITUTIVE MODELING OF PIEZOELECTRIC POLYMER COMPOSITES

Gregory M. Odegard[1]

ABSTRACT

A new modeling approach is proposed for predicting the bulk electromechanical properties of piezoelectric composites. The proposed model offers the same level of convenience as the well-known Mori-Tanaka method. In addition, it is shown to yield predicted properties that are, in most cases, more accurate or equally as accurate as the Mori-Tanaka scheme. In particular, the proposed method is used to determine the electromechanical properties of four piezoelectric polymer composite materials as a function of inclusion volume fraction. The predicted properties are compared to those calculated using the Mori-Tanaka and finite element methods.

1. INTRODUCTION

Piezoelectric materials are excellent candidates for use in sensors and actuators because of their ability to couple electrical and mechanical energy. For some applications, it is necessary to use composite materials in which one or more of the constituents have piezoelectric properties. To facilitate the design of these piezoelectric composite systems, convenient and accurate structure-property relationships must be developed.

Numerous attempts have been made to develop models to relate bulk electromechanical properties of composite materials to the electromechanical properties of individual constituents. Simple estimates, utilizing Voigt or Reuss-type approaches, have been used to predict the behavior of a limited class of composite geometries [1-4]. Upper and lower bounds for the electromechanical moduli have been determined [5-8]. Finite element analysis has also been used to predict electromechanical properties [9, 10]. Even though finite element analysis has the best potential for accurately predicting composite properties for any composite geometry, the solutions can be very expensive and time-consuming.

Several authors have extended Eshelby's [11] classical solution of an infinite medium containing a single ellipsoidal inclusion to include piezoelectric constituents [12-15]. Also referred to as the dilute solution, this approach ignores the interactions of the inclusions that occur at finite inclusion volume fractions. Other studies [14, 16-19] have focused on the classical extensions of Eshelby's solution for finite inclusion volume fractions, i.e., the Mori-Tanaka [20, 21], self-consistent [22, 23], and differential [24, 25] approaches. Analytical solutions for specific composite systems have also been determined [26-32]. Even though the overall framework of these approaches provides estimates for a wide range of inclusion sizes, geometries, and orientations, each of these methods suffers from drawbacks associated with the tradeoff between accuracy and computational convenience.

In this paper, a model is proposed for predicting the coupled electromechanical properties of piezoelectric composites. This model is an extension of a technique originally developed for predicting mechanical properties of composites by generalizing the Mori-Tanaka and self-consistent approaches [33]. It is shown that the method is as computationally convenient as the

---

[1] Staff Scientist, National Institute of Aerospace (NIA), 144 Research Drive, Hampton, VA 23666 (email: g.m.odegard@larc.nasa.gov)

Mori-Tanaka approach, and the predicted electromechanical properties of four piezoelectric composites computed using this model compare favorably to those obtained using the finite element method. First, the overall constitutive modeling of piezoelectric materials is discussed, followed by a description of the proposed model. Finally, the electromechanical properties of the four different piezoelectric composite systems are predicted using the proposed, Mori-Tanaka, and finite element models. The four piezoelectric composite systems used in this study were chosen to represent a wide range of practical materials: a graphite/Poly(vinylidene fluoride) (PVDF) composite, a Silicon Carbide (SiC)/PVDF particulate composite, a fibrous Lead Zirconate Titanate (PZT)/polyimide composite, and a PZT/polyimide particulate composite.

2. CONSTITUENT MATERIALS

The properties of constituent materials of the four piezoelectric composites are described below. The four composite materials used in the current study where chosen so that both spherical and fiberous inclusions were modeled in composites with a piezoelectric matrix and non-piezoelectric reinforcement, and a piezoelectric reinforcement with a non-piezoelectric matrix.

2.1. Polymer matrix materials

PVDF is a orthotropic, semi-crystalline polymer which exhibits a piezoelectric effect with an electric field applied along the 3-axis. Typical electromechanical properties of PVDF are given in Table 1. LaRC-SI is a thermoplastic polyimide that was developed for aerospace applications. The properties of LaRC-SI used in this study correspond to those determined at room temperature [34] and are also shown in Table 1.

2.2. Inclusion materials

In this study, the PVDF polymer was reinforced with infinitely-long graphite fibers and spherical SiC particles. The fibers were unidirectionally aligned along the PVDF 1-axis. The LaRC-SI polymer was reinforced with both infinitely-long PZT-7A fibers and spherical PZT-7A particles. PZT-7A is a ceramic that exhibits a piezoelectric effect with electric fields applied along all three principle axes. The PZT-7A fibers were unidirectionally aligned with the fiber 3-axis as the fiber-length axis. All of the inclusion electromechanical properties are given in Table 1.

3. MICROMECHANICS MODELING

3.1. Piezoelectric materials

There are three standard notation systems that are commonly used to describe the constitutive modeling of linear-piezoelectric materials [14]. Using the conventional indicial notation in which repeated subscripts are summed over the range of $i,j,m,n = 1,2,3$, the constitutive equations are

$$\sigma_{ij} = C_{ijmn}\varepsilon_{mn} + e_{nij}E_n$$
$$D_i = e_{imn}\varepsilon_{mn} - \kappa_{in}E_n \tag{1}$$

where σ_{ij}, ε_{ij}, E_i, and D_i are the stress tensor, strain tensor, electric field vector, and the electric displacement vector, respectively. C_{ijmn}, e_{nij}, and κ_{in} are the elastic stiffness tensor, the piezoelectric tensor, and the permittivity tensor, respectively. The divergence equations, which are the elastic equilibrium and Gauss' law, are, respectively,

$$\sigma_{ij,j} = 0$$
$$D_{i,i} = 0 \tag{2}$$

where the subscripted comma denotes partial differentiation. The gradient equations, which are the strain-displacement equations and electric field-potential, are, respectively,

$$\varepsilon_{ij} = \frac{1}{2}\left(u_{i,j} + u_{j,i}\right)$$
$$E_i = -\phi_{,i} \tag{3}$$

where u_i and ϕ are the mechanical displacement and electric potential, respectively.

In the modeling of piezoelectric materials, it is more convenient to restate Eqn. (1) so that the elastic and electric variables are combined to yield a single constitutive equation. This notation is identical to the conventional indicial notation with the exception that lower case subscripts retain the range of 1-3 and capitalized subscripts take on the range of 1-4, with repeated capitalized subscripts summed over 1-4. In this notation, Eqn. (1) is

$$\Sigma_{iJ} = E_{iJMn}Z_{Mn} \tag{4}$$

where Σ_{ij}, E_{iJMn}, and Z_{Mn} are, respectively,

$$\Sigma_{iJ} = \begin{cases} \sigma_{ij} & J = 1,2,3 \\ D_i & J = 4 \end{cases} \tag{5}$$

$$E_{iJMn} = \begin{cases} C_{ijmn} & J,M = 1,2,3 \\ e_{nij} & J = 1,2,3; M = 4 \\ e_{imn} & J = 4; M = 1,2,3 \\ -\kappa_{in} & J,M = 4 \end{cases} \tag{6}$$

$$Z_{Mn} = \begin{cases} \varepsilon_{mn} & M = 1,2,3 \\ E_n & M = 4 \end{cases} \tag{7}$$

The piezoelectric constitutive equation can be further simplified by expressing Eqn. (4) in matrix notation

$$\mathbf{\Sigma} = \mathbf{EZ} \tag{8}$$

where the boldface indicates either a 9×9 matrix ($\mathbf{E}$) or a 9×1 column vector ($\mathbf{\Sigma}$, $\mathbf{Z}$)

$$\mathbf{\Sigma}^t = \begin{bmatrix} \sigma_{11} & \sigma_{22} & \sigma_{33} & \sigma_{23} & \sigma_{13} & \sigma_{12} & | & D_1 & D_2 & D_3 \end{bmatrix} \tag{9}$$

$$\mathbf{Z}^t = \begin{bmatrix} \varepsilon_{11} & \varepsilon_{22} & \varepsilon_{33} & \gamma_{23} & \gamma_{13} & \gamma_{12} & | & E_1 & E_2 & E_3 \end{bmatrix} \tag{10}$$

$$\mathbf{E} = \left[\begin{array}{c|c} \mathbf{C} & \mathbf{e}^t \\ (6\times6) & (6\times3) \\ \hline \mathbf{e} & -\mathbf{\kappa} \\ (3\times6) & (3\times3) \end{array} \right] \tag{11}$$

In Eqn. (11), $\mathbf{C}$, $\mathbf{e}$, and $\mathbf{\kappa}$ denote the elastic stiffness matrix, the piezoelectric constant matrix, and the permittivity matrix, respectively. The superscript t denotes a matrix transposition. Note that $\gamma_{ij} = 2\varepsilon_{ij}$ in order to keep $\mathbf{E}$ a symmetric matrix. From Eqns (8) - (11), the constitutive equation for an orthotropic piezoelectric material is

$$\begin{bmatrix} \sigma_{11} \\ \sigma_{22} \\ \sigma_{33} \\ \sigma_{23} \\ \sigma_{13} \\ \sigma_{12} \\ \hline D_1 \\ D_2 \\ D_3 \end{bmatrix} = \left[\begin{array}{cccccc|ccc} C_{11} & C_{12} & C_{13} & 0 & 0 & 0 & 0 & 0 & e_{31} \\ C_{12} & C_{22} & C_{23} & 0 & 0 & 0 & 0 & 0 & e_{32} \\ C_{13} & C_{23} & C_{33} & 0 & 0 & 0 & 0 & 0 & e_{33} \\ 0 & 0 & 0 & C_{44} & 0 & 0 & 0 & e_{15} & 0 \\ 0 & 0 & 0 & 0 & C_{55} & 0 & e_{15} & 0 & 0 \\ 0 & 0 & 0 & 0 & 0 & C_{66} & 0 & 0 & 0 \\ \hline 0 & 0 & 0 & 0 & e_{15} & 0 & -\kappa_1 & 0 & 0 \\ 0 & 0 & 0 & e_{15} & 0 & 0 & 0 & -\kappa_2 & 0 \\ e_{31} & e_{32} & e_{33} & 0 & 0 & 0 & 0 & 0 & -\kappa_3 \end{array} \right] \begin{bmatrix} \varepsilon_{11} \\ \varepsilon_{22} \\ \varepsilon_{33} \\ \gamma_{23} \\ \gamma_{13} \\ \gamma_{12} \\ \hline E_1 \\ E_2 \\ E_3 \end{bmatrix} \tag{12}$$

where the contracted Voigt notation is used. In Eqn. (12), the 3-axis is aligned with the principle direction of polarization.

3.2. Electromechanical properties of composites

Using the direct approach [14, 35, 36] for the estimate of overall properties of heterogeneous materials, the volume-averaged piezoelectric fields of the composite with a total of N phases are

$$\overline{\Sigma} = \sum_{r=1}^{N} c_r \overline{\Sigma}_r \tag{13}$$

$$\overline{\mathbf{Z}} = \sum_{r=1}^{N} c_r \overline{\mathbf{Z}}_r \tag{14}$$

where c_r is the volume fraction of phase r, the overbar denotes a volume-averaged quantity, the subscript r denotes the phase, and $r = 1$ is the matrix phase. The constitutive equation for each phase is given by Eqn. (8). For a piezoelectric composite subjected to homogeneous elastic strain and electric field boundary conditions, $\mathbf{Z}^0$, it has been shown that $\overline{\mathbf{Z}} = \mathbf{Z}^0$ [16]. The constitutive equation for the piezoelectric composite can be expressed in terms of the volume-averaged fields

$$\overline{\Sigma} = \mathrm{E}\overline{\mathbf{Z}} \tag{15}$$

The volume-average strain and electric field in phase r is

$$\overline{\mathbf{Z}}_r = \mathbf{A}_r \overline{\mathbf{Z}} \tag{16}$$

where $\mathbf{A}_r$ is the concentration tensor of phase r, and

$$\sum_{r=1}^{N} c_r \mathbf{A}_r = \mathbf{I} \tag{17}$$

where $\mathbf{I}$ is the identity tensor. Combining Eqns. (13)-(17) yields the electromechanical modulus of the composite in terms of the constituent moduli

$$\mathbf{E} = \mathbf{E}_1 + \sum_{r=2}^{N} c_r \left(\mathbf{E}_r - \mathbf{E}_1 \right) \mathbf{A}_r \tag{18}$$

Various procedures exist for evaluating the concentration tensor. The most widely used approaches are the Mori-Tanaka, self-consistent and differential schemes.

For the Mori-Tanaka approach, the concentration tensor is

$$\mathbf{A}_s = \mathbf{A}_r^{dil} \left[c_1 \mathbf{I} + \sum_{r=2}^{N} c_r \mathbf{A}_r^{dil} \right]^{-1} \tag{19}$$

where $\mathbf{A}_r^{dil}$ is the dilute concentration tensor given by

$$\mathbf{A}_r^{dil} = \left[\mathbf{I} + \mathbf{S}_r \mathbf{E}_1^{-1} \left(\mathbf{E}_r - \mathbf{E}_1 \right) \right]^{-1} \tag{20}$$

In Eqn. (20) $\mathbf{S}_r$ is the constraint tensor for phase r, which is analogous to the Eshelby tensor used in determining elastic properties of composite materials [11]. The constraint tensor is evaluated as a function of the lengths of the principle axes of the reinforcing phase r, a_i^r, and the electromechanical properties of the surrounding matrix

$$\mathbf{S}_r = f\left(\mathbf{E}_1, a_1^r, a_2^r, a_3^r\right) \tag{21}$$

The complete expression for Eqn. (21) is given elsewhere [16]. While the Mori-Tanaka approach provides for a quick and simple calculation of the bulk composite electromechanical properties, it has been shown that it yields predicted mechanical properties that are relatively low and high for composites with stiffer inclusions and matrix, respectively [33]. This issue could possibly lead to less accurate estimations of the electromechanical moduli, especially for relatively large inclusion volume fractions [37-39].

In the self-consistent and differential schemes, the concentration tensor is

$$\mathbf{A}_r = \left[\mathbf{I} + \mathbf{S}_r \mathbf{E}^{-1}\left(\mathbf{E}_r - \mathbf{E}\right)\right]^{-1} \tag{22}$$

where $\mathbf{E}$ is the unknown electromechanical moduli of the composite, and the constraint tensor, $\mathbf{S}_r$, is evaluated as a function of $\mathbf{E}$ and a_i^r. Since the electromechanical moduli of the composite appears in both Eqns. (22) and (18), iterative schemes or numerical techniques are ultimately required for the prediction of the electromechanical moduli of composites using the self-consistent and differential approaches. This approach results in slow and complicated calculations.

It has been demonstrated [33] that a more general form of the concentration tensor can be used for the prediction of mechanical properties of composites. Extending this concept to the prediction of electromechanical properties results in

$$\mathbf{A}_r = \left[\mathbf{I} + \mathbf{S}_r \mathbf{E}_0^{-1}\left(\mathbf{E}_r - \mathbf{E}_0\right)\right]^{-1} \tag{23}$$

where $\mathbf{E}_0$ is the electroelastic moduli of the reference medium, and the constraint tensor is evaluated using $\mathbf{E}_0$ and a_i^r. Therefore, it is assumed that the reference medium is the material that immediately surrounds the inclusion for the evaluation of the constraint and concentration tensors. Naturally, the electroelastic moduli of the reference medium can have a wide range of values, however, it is most realistic to assume that they are similar to the moduli of the overall composite, as is the case in the self-consistent and differential methods.

For convenience, a simple, yet accurate, estimation of the overall electroelastic moduli can be chosen for the reference medium so that the overall properties of the piezoelectric composite can be calculated using Eqns. (18) and (23). Thus, the straightforward computation of the moduli can be achieved, as with the Mori-Tanaka approach, but with an accuracy similar to the self-consistent and differential methods. Even though a simple and accurate estimation of the reference medium means that the electroelastic moduli can be calculated without Eqns. (18) and (23), this framework allows for an accurate computation of the moduli for various inclusion sizes, geometries, and orientations.

The reference medium is approximated with a set of equations that are similar to the Halpin-Tsai relation [40], which is extended here for multiple inclusions and piezoelectric composites

$$E_{iJKl}^0 = E_{iJKl}^1 \frac{1 + \sum_{r=2}^{N} \eta_{iJKl}^r c_r}{1 - \sum_{r=2}^{N} \eta_{iJKl}^r c_r} \tag{24}$$

where

$$\eta_{iJKl}^r = \frac{E_{iJKl}^r - E_{iJKl}^1}{E_{iJKl}^r + E_{iJKl}^1} \tag{25}$$

Eqns. (24) and (25) indicate that as $c_1 \rightarrow 1$ and $c_r \rightarrow 1$, $E_{iJKl}^0 \rightarrow E_{iJKl}^1$ and $E_{iJKl}^0 \rightarrow E_{iJKl}^r$, respectively.

Eqns. (18) and (23)-(25) were used to calculate the electromechanical properties for the four composite systems for inclusion volume fractions ranging from 0% to the maximum theoretical limits, which are 90% and 75% for fibrous and particulate composites, respectively. The constraint tensor in Eqn. (23) was evaluated numerically using Gaussian quadrature [41]. The fibers were modeled as infinitely long cylinders and the particles were modeled as spheres. Perfect bonding between the inclusions and matrix was assumed.

4. FINITE ELEMENT ANALYSIS

Another approach to estimate the electromechanical properties of piezoelectric composites is using finite element analysis of a representative volume element (RVE) of the material. Whereas the methods of the previous section provide relatively quick predictions by assuming that the stress and strain fields inside the inclusions are constant, finite element analysis predicts these fields in the inclusion and matrix, and thus, provides a more realistic prediction to the overall electromechanical moduli of the composite. This added accuracy comes at a price, however, since each independent property of the piezoelectric composite (16 independent parameters are shown in Eqn. (12)) must be determined by a single finite element analysis. In parametric studies where the many combinations of inclusion shape and volume fraction must be considered, the finite element approach can become very time-consuming and expensive. Therefore, in this study, the finite element results are used to check the accuracy of the modeling methods discussed in the previous section.

The finite element model was developed and executed using ANSYS® 7.0. Representative volume elements (RVEs) of fiber- and particulate-reinforced composites were meshed using 10-noded electromechanical tetrahedral elements with 40 degrees of freedom, three displacements and a voltage at each node (SOLID98). The RVEs are shown in Figs. 1 and 2. The top portion of the two figures shows the outside mesh of the RVE, and the bottom shows the mesh of the inclusion with a transparent matrix. The fibrous composite RVE simulates a hexagonal packing arrangement, with a maximum fiber volume fraction of about 90%. The particulate composite RVE has hexagonal packing in one plane with with a maximum particle

volume fraction of about 60%. For each finite element analysis, the desired volume fraction was obtained by adjusting the dimensions of the RVE while keeping the reinforcement size constant. The properties of the materials are shown in Table 1.

For homogeneous applied elastic strains and electric fields, the displacements and voltages on the boundary of the RVEs were, respectively,

$$
\begin{aligned}
u_i(B) &= \varepsilon_{ij} x_j \\
\phi(B) &= -E_i x_i
\end{aligned}
\tag{26}
$$

where B indicates the boundary of the RVE. A total of 16 boundary conditions were applied to the finite element models for each combination of material type and volume fraction. Each boundary condition was used to predict one of the independent boundary conditions shown in Eqn. (12). The elastic constants and the corresponding applied strains, electric fields, and the boundary conditions calculated using Eqn. (26) are listed in Tables 2 to 6. All unspecified strains and electric fields in Tables 2 to 6 are zero.

The elastic strain energy, dielectric energy, and electromechanical energy are, respectively,

$$
\begin{aligned}
U_e &= \frac{V}{2} C_{ijkl} \varepsilon_{ij} \varepsilon_{kl} \\
U_d &= \frac{V}{2} \kappa_{ij} E_i E_j \\
U_{em} &= \frac{V}{2} e_{ijk} \varepsilon_{jk} E_i
\end{aligned}
\tag{27}
$$

where V is the volume of the RVE. These quantities where calculated for the appropriate boundary conditions as shown in Tables 2 to 6. The corresponding elastic constants were calculated using Eqn. (27) and the summation of the elastic strain energy, dielectric energy, and electromechanical energies for all of the elements in each finite element analysis.

5. RESULTS

The Young's moduli, Y_1, Y_2, and Y_3; shear moduli, G_{23}, G_{13}, and G_{12}; piezoelectric constants, e_{15}, e_{31}, e_{32}, e_{33}; and dielectric constants, κ_1/κ_0, κ_2/κ_0, and κ_3/κ_0; for the four materials discussed in this paper are presented below. The subscripts of these quantities indicate the corresponding axes, as shown in Eqn. (12), and the permittivity of free space, κ_0, is 8.85×10^{-12} C/m^2.

5.1. Graphite/PVDF fiber composite

The Young's moduli of the graphite/PVDF composite are shown in Fig. 3 as a function of the graphite fiber volume fraction for the results obtained with the finite element analysis, the proposed model discussed above, and the Mori-Tanaka method. For the Young's modulus parallel to the fiber-alignment direction, Y_1, all three models predict the same values for the entire range of fiber volume fractions. For the two transverse moduli, Y_2 and Y_3, the proposed

and finite element models match very well for the entire range of fiber volume fractions, while the Mori-Tanaka under-predicts the Young's moduli.

The shear moduli of this material for the entire range of fiber volume fractions are shown in Fig. 4. For the longitudinal shear moduli, G_{13} and G_{12}, the proposed model has a closer agreement with the finite element model than the Mori-Tanaka model has with the finite element model. The transverse shear modulus, G_{23}, is nearly equal for all three models over the range of fiber volume fractions.

The piezoelectric constants, e_{31}, e_{32}, and e_{33}, are shown in Fig. 5 as a function of the fiber volume fraction. The three models predict nearly equal values of e_{31} and e_{32} over the entire range. For the piezoelectric constant e_{32}, the proposed and Mori-Tanaka results over-predict and under-predict the finite element model, respectively. At a fiber volume fraction of 90%, the proposed model shows close agreement with the finite element model.

The dielectric constants, κ_1/κ_0, κ_2/κ_0, and κ_3/κ_0, are shown in Fig. 6. All three models predict identical values for all three dielectric constants for the complete range of fiber volume fractions.

5.2. SiC/PVDF particle composite

The Young's moduli of the SiC/PVDF composite are shown in Fig.7 as a function of particle volume fraction. The trends for all three Young's moduli are similar. At particle volume fractions of about 40% and lower, all three models predict nearly identical moduli. At higher particle volume fractions, the finite element model predicts moduli that are larger than the proposed and Mori-Tanaka models, especially at a particle volume fraction of 60%. At the larger volume fractions, the proposed model predicts moduli that have closer agreement with the finite element results than has the predicted values from the Mori-Tanaka model.

The three shear moduli are shown in Fig. 8 for the entire range of particle volume fractions. For all three shear moduli, at volume fractions below 60%, the Mori-Tanaka and finite element models have close agreement, with the proposed model over-predicting the shear moduli. For a volume fraction of 60%, the shear moduli of the finite element model start increasing dramatically, and the proposed model shows closer agreement with the finite element model than does the Mori-Tanaka approach.

The piezoelectric constants are shown in Fig. 9 as a function of particle volume fraction. For all three piezoelectric constants, there is close agreement between all three models for the entire range of volume fractions.

The three dielectric constants for the composite are shown in Fig. 10. Similar to the graphite/PVDF composite, all three models predict identical values for all three dielectric constants for the entire range of particle volume fractions.

5.3. PZT-7A/polyimide fiber composite

The Young's moduli of the PZT-7A composite are shown in Fig. 11 for the entire range of fiber volume fractions. For the longitudinal Young's modulus, Y_3, all three models predict the same values over the complete range of volume fractions. For the transverse Young's moduli, Y_1 and Y_2, the proposed and finite element models have close agreement, while the Mori-Tanaka significantly under-predicts the finite element model, especially at volume fractions above 40%.

The shear moduli of the composite are plotted as a function of fiber volume fraction in Fig. 12. For the longitudinal shear moduli, G_{23} and G_{13}, The Mori-Tanaka and finite element models show close agreement, particularly at low volume fractions and at 90% volume fraction. For the entire range of fiber volume fraction, the proposed model over-predicts the finite element data. However, for the transverse shear moduli, G_{12}, the proposed model shows good agreement with the finite element model while the Mori-Tanaka approach significantly under-predicts the finite element data.

The piezoelectric constants of this material are shown in Fig. 13. For the constants $e_{31} = e_{32}$ and e_{33}, all three models predict very similar values for the entire range of fiber volume fractions. For e_{15}, both the proposed and Mori-Tanaka models under-predict the finite element model, especially at a volume fraction of 90%.

The dielectric constants are shown in Fig. 14 as a function of fiber volume fraction. For the transverse dielectric constants, κ_1/κ_0 and κ_2/κ_0, the proposed model predicts the finite element model data better than does the Mori-Tanka model, especially for fiber volume fractions above 60%. For the longitudinal dielectric constant, κ_3/κ_0, the three models predict identical values over the entire range of volume fractions.

5.4. PZT-7A/polyimide particle composite

The Young's moduli of the PZT-7A/LaRC-SI particulate composite are shown in Fig. 15 as a function of particle volume fraction. For both the transverse Young's moduli, Y_1 and Y_2, and the longitudinal Young's modulus, Y_3, the proposed model agrees closely with the finite element model up to a particle volume fraction of about 40%. For larger particle volume fractions, the finite element data are significantly larger. The Mori-Tanaka model significantly under-predicts the finite element data for volume fractions above 30%.

The shear moduli of this material for the range of volume fractions are shown in Fig. 16. For the longitudinal shear moduli, G_{23} and G_{13}, the proposed and Mori-Tanaka models both predict values that are close to the finite element model up to a particle volume fraction of 30%. For higher particle volume fractions, the proposed model has better agreement with the finite element data than has the Mori-Tanaka model. For the longitudinal shear modulus, the Mori-Tanaka model agrees very closely with the finite element model up to a particle volume fraction of 50%. For higher particle volume fractions, the proposed model shows closer agreement to the finite element model than does the Mori-Tanaka model.

The piezoelectric constants are shown in Fig. 17 as a function of particle volume fraction. For all four constants, e_{15}, $e_{31} = e_{32}$, and e_{33}, all three models shown close agreement up to a particle volume fraction of 40%. For larger volume fractions, the finite element data diverge quickly from the proposed and Mori-Tanaka models, with the proposed model showing closer agreement.

The dielectric constants of the material are shown in Fig. 18. For the transverse dielectric constants, κ_1/κ_0 and κ_2/κ_0, and the longitudinal dielectric constant, κ_3/κ_0, the predicted values from the Mori-Tanaka model agree with the finite element model up to a particle volume fraction of about 40%. Above that value, the Mori-Tanaka model significantly under-predicts the finite element data. The proposed exhibits better agreement with the finite element model above particle volume fractions of 50%.

6. SUMMARY

A new modeling approach has been proposed for predicting the bulk electromechanical properties of piezoelectric composites. The proposed model offers the same level of convenience as the Mori-Tanaka method, that is, it does not require iterative or numerical schemes for obtaining the predicted properties, as is required with the self-consistent and differential schemes. In addition, it has been shown to yield predicted properties that are, in most cases, more accurate or equally as accurate as the Mori-Tanaka method. In particular, the proposed method has been used to determine the electromechanical properties of four piezoelectric composite materials as a function of volume fraction: a graphite/ PVDF composite, a SiC/PVDF particulate composite, a fibrous PZT-7A/LaRC-SI composite, and a PZT-7A/LaRC-SI particulate composite. The predicted properties have been compared to those calculated using the Mori-Tanaka and finite element methods.

REFERENCES

[1] Newnham, R.E.; Skinner, D.P., and Cross, L.E.: Connectivity and Piezoelectric-Pyroelectric Composites. *Materials Research Bulletin*. Vol. 13, 1978, pp. 525-536.

[2] Banno, H.: Recent Developments of Piezoelectric Ceramic Products and Composites of Synthetic Rubber and Piezoelectric Ceramic Particles. *Ferroelectrics*. Vol. 50, 1983, pp. 329-338.

[3] Chan, H.L.W. and Unsworth, J.: Simple Model for Piezoelectric Ceramic/Polymer 1-3 Composites Used in Ultrasonic Transducer Applications. *IEEE Transactions on Ultrasonics, Ferroelectrics, and Frequency Control*. Vol. 36, 1989, pp. 434-441.

[4] Smith, W.A. and Auld, B.A.: Modeling 1-3 Composite Piezoelectrics: Thickness-Mode Oscillations. *IEEE Transactions on Ultrasonics, Ferroelectrics, and Frequency Control*. Vol. 38, 1991, pp. 40-47.

[5] Olson, T. and Avellaneda, M.: Effective Dielectric and Elastic Constants of Piezoelectric Polycrystals. *Journal of Applied Physics*. Vol. 71, 1992, pp. 4455-4464.

[6] Bisegna, P. and Luciano, R.: Variational Bounds for the Overall Properties of Piezoelectric Composites. *Journal of the Mechanics and Physics of Solids*. Vol. 44, 1996, pp. 583-602.

[7] Hori, M. and Nemat-Nasser, S.: Universal Bounds for Effective Piezoelectric Moduli. *Mechanics of Materials*. Vol. 30, 1998, pp. 1-19.

[8] Li, J.Y. and Dunn, M.L.: Variational Bounds for the Effective Moduli of Heterogeneous Piezoelectric Solids. *Philosophical Magazine, A: Physics of Condensed Matter, Structure, Defects, and Mechanical Properties*. Vol. 81, 2001, pp. 903-926.

[9]   Gaudenzi, P.: On the Electromechanical Response of Active Composite Materials with Piezoelectric Inclusions. *Computers and Structures*. Vol. 65, 1997, pp. 157-168.

[10]   Poizat, C. and Sester, M.: Effective Properties of Composites with Embedded Piezoelectric Fibres. *Computational Materials Science*. Vol. 16, 1999, pp. 89-97.

[11]   Eshelby, J.D.: The Determination of the Elastic Field of an Ellipsoidal Inclusion, and Related Problems. *Proceedings of the Royal Society of London, Series A*. Vol. 241, 1957, pp. 376-396.

[12]   Wang, B.: Three-Dimensional Analysis of an Ellipsoidal Inclusion in a Piezoelectric Material. *International Journal of Solids and Structures*. Vol. 29, 1992, pp. 293-308.

[13]   Benveniste, Y.: The Determination of the Elastic and Electric Fields in a Piezoelectric Inhomogeneity. *Journal of Applied Physics*. Vol. 72, 1992, pp. 1086-1095.

[14]   Dunn, M.L. and Taya, M.: Micromechanics Predictions of the Effective Electroelastic Moduli of Piezoelectric Composites. *International Journal of Solids and Structures*. Vol. 30, No. 2, 1993, pp. 161-175.

[15]   Chen, T.: An Invariant Treatment of Interfacial Discontinuities in Piezoelectric Media. *International Journal of Engineering Science*. Vol. 31, 1993, pp. 1061-1072.

[16]   Dunn, M.L. and Taya, M.: An Analysis of Piezoelectric Composite Materials Containing Ellipsoidal Inhomogeneities. *Proceedings of the Royal Society of London, Series A*. Vol. 443, 1993, pp. 265-287.

[17]   Chen, T.: Micromechanical Estimates of the Overall Thermoelectroelastic Moduli of Multiphase Fibrous Composites. *International Journal of Solids and Structures*. Vol. 31, 1994, pp. 3099-3111.

[18]   Huang, J.H. and Kuo, W.S.: Micromechanics Determination of the Effective Properties of Piezoelectric Composites Containing Spatially Oriented Short Fibers. *Acta Materialia*. Vol. 44, 1996, pp. 4889-4898.

[19]   Fakri, N.; Azrar, L., and El Bakkali, L.: Electroelastic Behavior Modeling of Piezoelectric Composite Materials Containing Spatially Oriented Reinforcements. *International Journal of Solids and Structures*. Vol. 40, 2003, pp. 361-384.

[20]   Mori, T. and Tanaka, K.: Average Stress in Matrix and Average Elastic Energy of Materials with Misfitting Inclusions. *Acta Metallurgica*. Vol. 21, 1973, pp. 571-574.

[21]   Benveniste, Y.: A New Approach to the Application of Mori-Tanaka's Theory in Composite Materials. *Mechanics of Materials*. Vol. 6, 1987, pp. 147-157.

[22]   Hill, R.: A Self-Consistent Mechanics of Composite Materials. *Journal of the Mechanics and Physics of Solids*. Vol. 13, 1965, pp. 213-222.

[23]   Budiansky, B.: On the Elastic Moduli of Some Heterogeneous Materials. *Journal of the Mechanics and Physics of Solids*. Vol. 13, 1965, pp. 223-227.

[24]   McLaughlin, R.: A Study of the Differential Scheme for Composite Materials. *International Journal of Engineering Science*. Vol. 15, 1977, pp. 237-244.

[25]   Norris, A.N.: A Differential Scheme for the Effective Moduli of Composites. *Mechanics of Materials*. Vol. 4, 1985, pp. 1-16.

[26]   Dunn, M.L.: Electroelastic Green's Functions for Transversely Isotropic Piezoelectric media and Their Application to the Solution of Inclusion and Inhomogeneity Problems. *International Journal of Engineering Science*. Vol. 32, No. 1, 1994, pp. 119-131.

[27]   Wang, B.: Effective Behavior of Piezoelectric Composites. *Applied Mechanics Reviews*. Vol. 47, 1994, pp. S112-S121.

[28]   Dunn, M.L. and Wienecke, H.A.: Green's Functions for Transversely Isotropic Piezoelectric Solids. *International Journal of Solids and Structures*. Vol. 33, 1996, pp. 4571-4581.

[29]   Chen, T.: Effective Properties of Platelet Reinforced Piezocomposites. *Composites: Part B*. Vol. 27, 1996, pp. 467-474.

[30]   Dunn, M.L. and Wienecke, H.A.: Inclusions and Inhomogeneities in Transversely Isotropic Piezoelectric Solids. *International Journal of Solids and Structures*. Vol. 34, No. 27, 1997, pp. 3571-3582.

[31]   Mikata, Y.: Determination of Piezoelectric Eshelby Tensor in Transversely Isotropic Piezoelectric Solids. *International Journal of Engineering Science*. Vol. 38, 2000, pp. 605-641.

[32]   Mikata, Y.: Explicit Determination of Piezoelectric Eshelby Tensors for a Spheroidal Inclusion. *International Journal of Solids and Structures*. Vol. 38, 2001, pp. 7045-7063.

[33]   Dvorak, G.J. and Srinivas, M.V.: New Estimates of Overall Properties of Heterogeneous Solids. *Journal of the Mechanics and Physics of Solids*. Vol. 47, 1999, pp. 899-920.

[34]   Nicholson, L.M.; Whitley, K.S.; Gates, T.S., and Hinkley, J.A.: Influence of Molecular Weight on the Mechanical Performance of a Thermoplastic Glassy Polyimide. *Journal of Materials Science*. Vol. 35, No. 24, 2000, pp. 6111-6122.

[35]   Hill, R.: Elastic Properties of Reinforced Solids: Some Theoretical Principles. *Journal of the Mechanics and Physics of Solids*. Vol. 11, 1963, pp. 357-372.

[36] Dvorak, G.J. and Benveniste, Y.: On Transformation Strains and Uniform Fields in Multiphase Elastic Media. *Proceedings of the Royal Society of London, Series A*. Vol. 437, 1992, pp. 291-310.

[37] Christensen, R.M.: A Critical Evaluation for a Class of Micromechanics Models. *Journal of the Mechanics and Physics of Solids*. Vol. 38, 1990, pp. 379-404.

[38] Christensen, R.M.; Schantz, H., and Shapiro, J.: On the Range of Validity of the Mori-Tanaka Method. *Journal of the Mechanics and Physics of Solids*. Vol. 40, 1992, pp. 69-73.

[39] Benedikt, B.; Rupnowski, P., and Kumosa, M.: Visco-elastic Stress Distributions and Elastic Properties in Unidirectional Composites with Large Volume Fractions of Fibers. *Acta Materialia*. Vol. 51, No. 12, 2003, pp. 3483-3493.

[40] Halpin, J.C. and Tsai, S.W.: Environmental Factors in Composites Design. AFML-TR-67-423, 1967.

[41] Davis, P.J. and Polonsky, I.: Numerical Interpolation, Differentiation and Integration. In: *Handbook of Mathematical Functions with Formulas, Graphs, and Mathematical Tables*. M. Abramowitz and I. A. Stegun, eds. New York: John Wiley & Sons, 1972, pp. 875-924.

Table 1

Electromechanical properties of matrix and inclusion materials

Property	PVDF	LaRC-SI	Graphite fiber	SiC particle	PZT-7A
C_{11} (GPa)	3.8	8.1	243.7	483.7	148.0
C_{12} (GPa)	1.9	5.4	6.7	99.1	76.2
C_{13} (GPa)	1.0	5.4	6.7	99.1	74.2
C_{22} (GPa)	3.2	8.1	24.0	483.7	148.0
C_{23} (GPa)	0.9	5.4	9.7	99.1	74.2
C_{33} (GPa)	1.2	8.1	24.0	483.7	131.0
C_{44} (GPa)	0.7	1.4	11.0	192.3	25.4
C_{55} (GPa)	0.9	1.4	27.0	192.3	25.4
C_{66} (GPa)	0.9	1.4	27.0	1923	35.9
κ_1/κ_0	7.4	2.8	12.0	10.0	460.0
κ_2/κ_0	9.3	2.8	12.0	10.0	460.0
κ_3/κ_0	7.6	2.8	12.0	10.0	235.0
e_{15} (C/m^2)	0.0	0.0	0.0	0.0	9.2
e_{31} (C/m^2)	0.024	0.0	0.0	0.0	-2.1
e_{32} (C/m^2)	0.001	0.0	0.0	0.0	-2.1
e_{33} (C/m^2)	-0.027	0.0	0.0	0.0	9.5

Table 2
Boundary conditions for axial stiffness components

| Property	Applied strain and electric field	Displacements and electric potential	Elastic energy
C_{11}	$\varepsilon_{11} = \varepsilon$	$u_1(B) = \varepsilon x_1$ $u_2(B) = 0$ $u_3(B) = 0$ $\phi(B) = 0$	$U_e = \dfrac{V}{2} C_{11} \varepsilon^2$
C_{22}	$\varepsilon_{22} = \varepsilon$	$u_1(B) = 0$ $u_2(B) = \varepsilon x_2$ $u_3(B) = 0$ $\phi(B) = 0$	$U_e = \dfrac{V}{2} C_{22} \varepsilon^2$
C_{33}	$\varepsilon_{33} = \varepsilon$	$u_1(B) = 0$ $u_2(B) = 0$ $u_3(B) = \varepsilon x_3$ $\phi(B) = 0$	$U_e = \dfrac{V}{2} C_{33} \varepsilon^2$

Table 3
Boundary conditions for plane-strain bulk moduli

Property	Applied strain and electric field	Displacements and electric potential	Elastic energy
K_{23}	$\varepsilon_{22} = \varepsilon_{33} = \varepsilon$	$u_1(B) = 0$ $u_2(B) = \varepsilon x_2$ $u_3(B) = \varepsilon x_3$ $\phi(B) = 0$	$U_e = \dfrac{V}{2} K_{23} \varepsilon^2$
K_{13}	$\varepsilon_{11} = \varepsilon_{33} = \varepsilon$	$u_1(B) = \varepsilon x_1$ $u_2(B) = 0$ $u_3(B) = \varepsilon x_3$ $\phi(B) = 0$	$U_e = \dfrac{V}{2} K_{13} \varepsilon^2$
K_{12}	$\varepsilon_{11} = \varepsilon_{22} = \varepsilon$	$u_1(B) = \varepsilon x_1$ $u_2(B) = \varepsilon x_2$ $u_3(B) = 0$ $\phi(B) = 0$	$U_e = \dfrac{V}{2} K_{12} \varepsilon^2$

Table 4
Boundary conditions for shear stiffness components

Property	Applied strain and electric field	Displacements and electric potential	Elastic energy
C_{44}	$\varepsilon_{23} = \dfrac{\gamma}{2}$	$u_1(B) = 0$ $u_2(B) = (\gamma/2)x_3$ $u_3(B) = (\gamma/2)x_2$ $\phi(B) = 0$	$U_e = \dfrac{V}{2}C_{44}\gamma^2$
C_{55}	$\varepsilon_{13} = \dfrac{\gamma}{2}$	$u_1(B) = (\gamma/2)x_3$ $u_2(B) = 0$ $u_3(B) = (\gamma/2)x_1$ $\phi(B) = 0$	$U_e = \dfrac{V}{2}C_{55}\gamma^2$
C_{66}	$\varepsilon_{12} = \dfrac{\gamma}{2}$	$u_1(B) = (\gamma/2)x_2$ $u_2(B) = (\gamma/2)x_1$ $u_3(B) = 0$ $\phi(B) = 0$	$U_e = \dfrac{V}{2}C_{66}\gamma^2$

Table 5
Boundary conditions for dielectric constants

Property	Applied strain and electric field	Displacements and electric potential	Dielectric energy
κ_1/κ_0	$E_1 = E$	$u_1(B) = 0$ $u_2(B) = 0$ $u_3(B) = 0$ $\phi(B) = -Ex_1$	$U_d = \dfrac{V}{2}\kappa_1 E^2$
κ_2/κ_0	$E_2 = E$	$u_1(B) = 0$ $u_2(B) = 0$ $u_3(B) = 0$ $\phi(B) = -Ex_2$	$U_d = \dfrac{V}{2}\kappa_2 E^2$
κ_3/κ_0	$E_3 = E$	$u_1(B) = 0$ $u_2(B) = 0$ $u_3(B) = 0$ $\phi(B) = -Ex_3$	$U_d = \dfrac{V}{2}\kappa_3 E^2$

Table 6

Boundary conditions for piezoelectric constants

Property	Applied strain and electric field	Displacements and electric potential	Electromechanical energy
e_{15}	$\varepsilon_{13} = \dfrac{\gamma}{2}$ $E_1 = E$	$u_1(B) = (\gamma/2)x_3$ $u_2(B) = 0$ $u_3(B) = (\gamma/2)x_1$ $\phi(B) = -Ex_1$	$U_{em} = \dfrac{V}{2}e_{15}\gamma E$
e_{31}	$\varepsilon_{11} = \varepsilon$ $E_3 = E$	$u_1(B) = \varepsilon x_1$ $u_2(B) = 0$ $u_3(B) = 0$ $\phi(B) = -Ex_3$	$U_{em} = \dfrac{V}{2}e_{31}\varepsilon E$
e_{32}	$\varepsilon_{22} = \varepsilon$ $E_3 = E$	$u_1(B) = 0$ $u_2(B) = \varepsilon x_2$ $u_3(B) = 0$ $\phi(B) = -Ex_3$	$U_{em} = \dfrac{V}{2}e_{32}\varepsilon E$
e_{33}	$\varepsilon_{33} = \varepsilon$ $E_3 = E$	$u_1(B) = 0$ $u_2(B) = 0$ $u_3(B) = \varepsilon x_3$ $\phi(B) = -Ex_3$	$U_{em} = \dfrac{V}{2}e_{33}\varepsilon E$
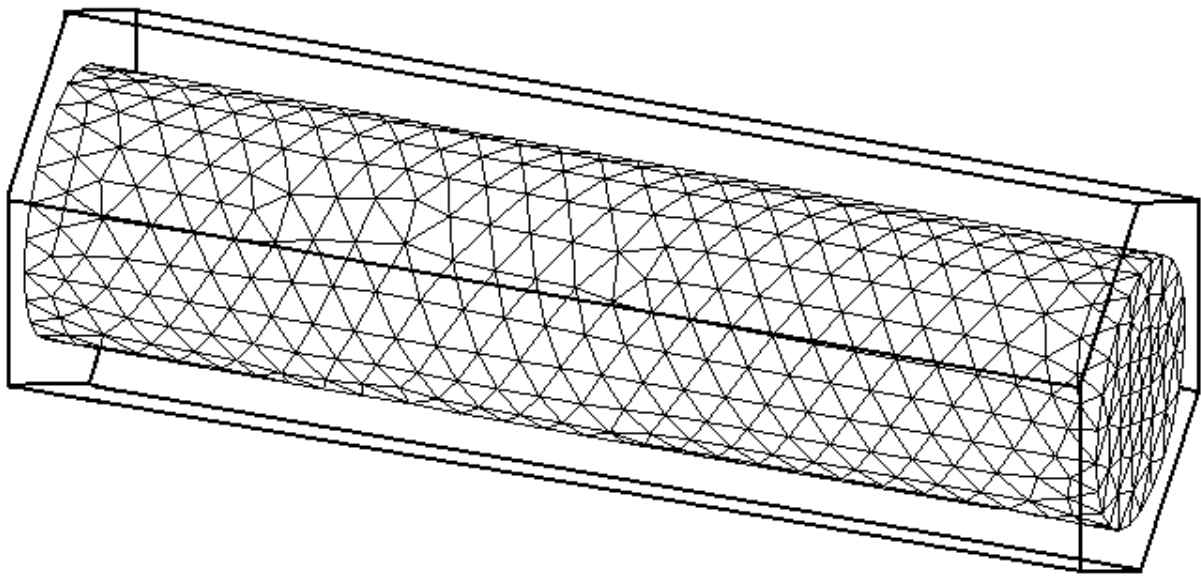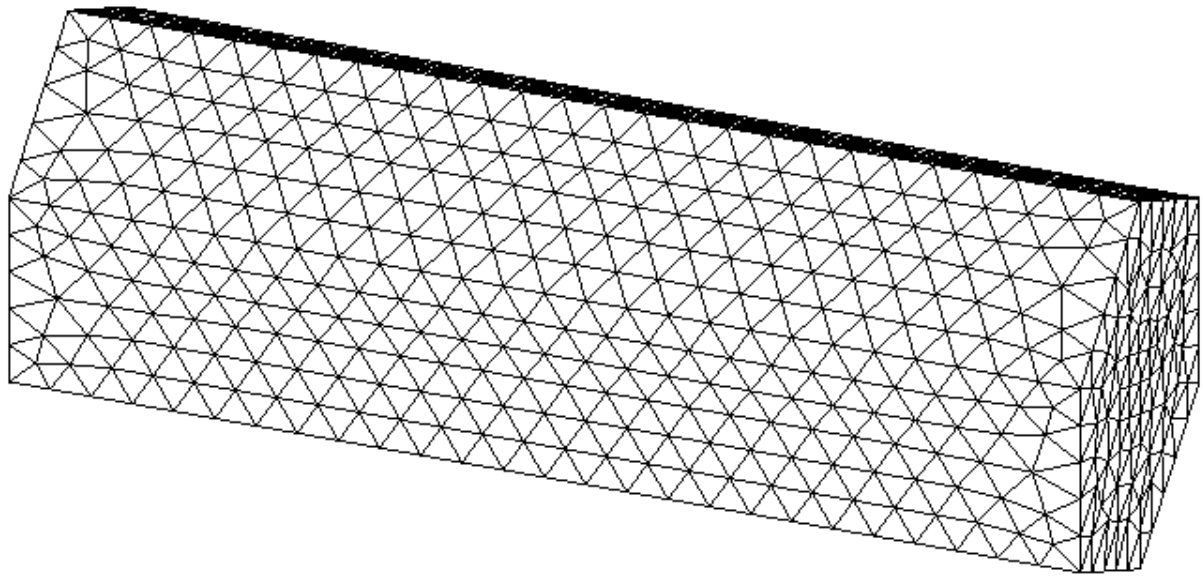
Figure 1. *Finite element RVE of fiber composite*
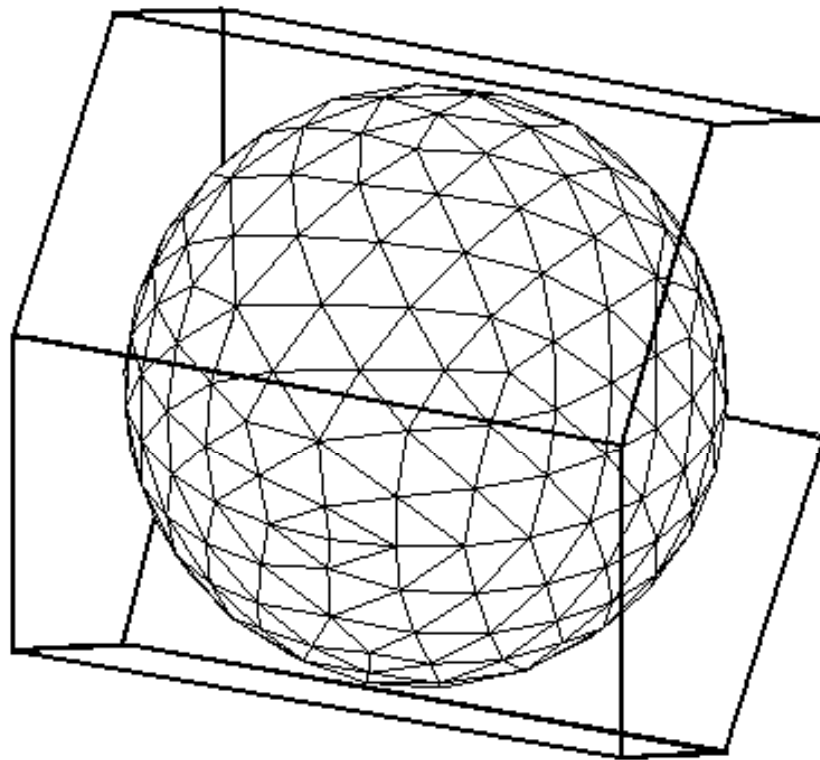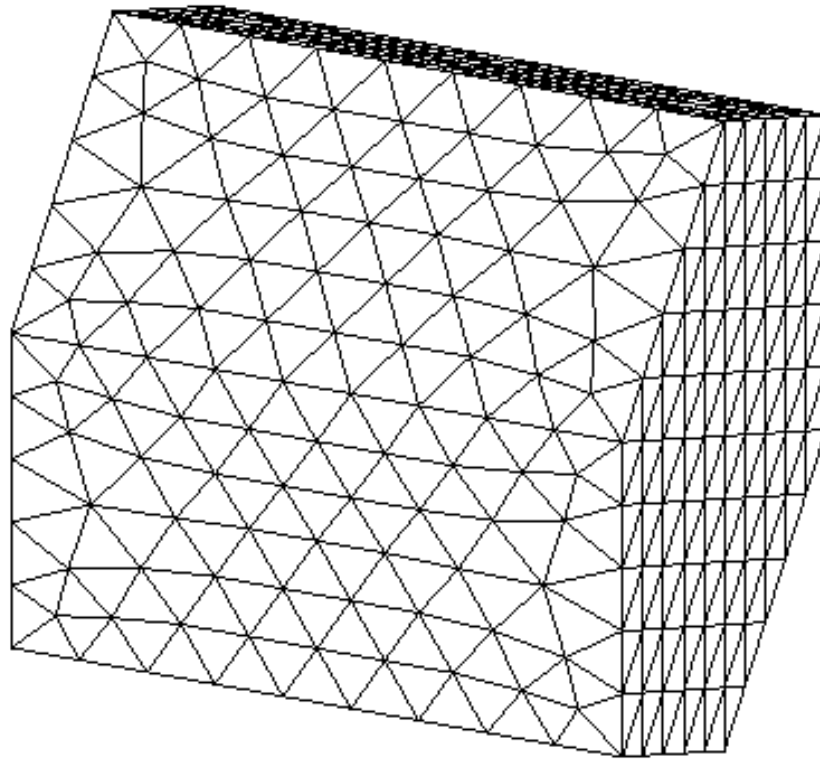
Figure 2. *Finite element RVE of particle composite*
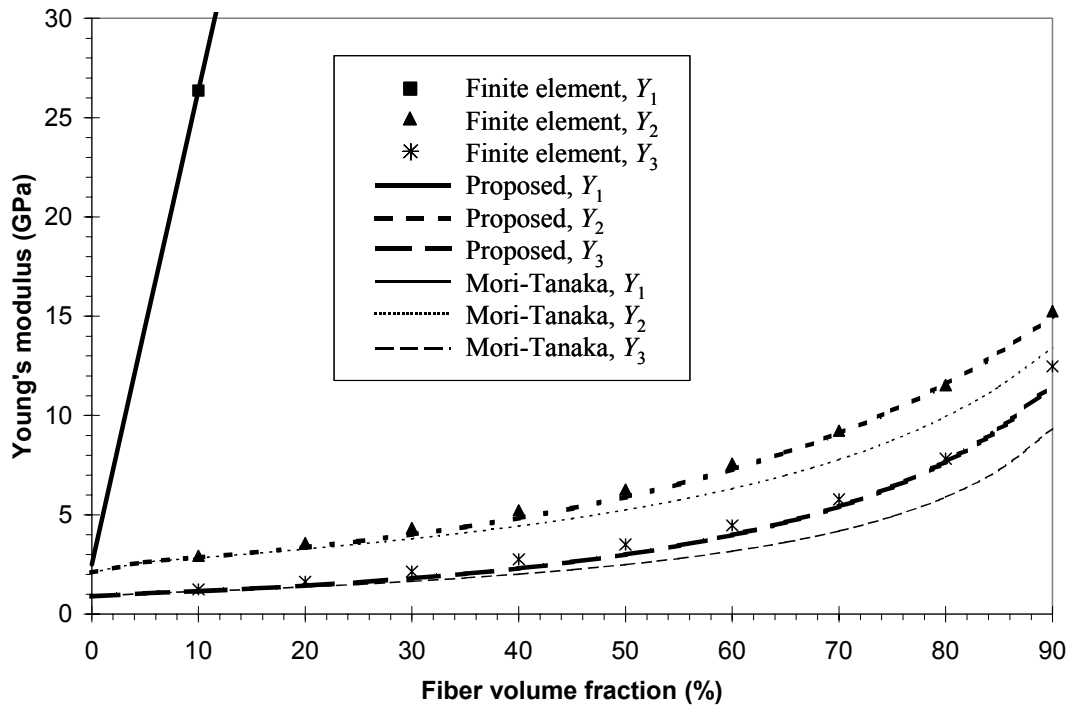
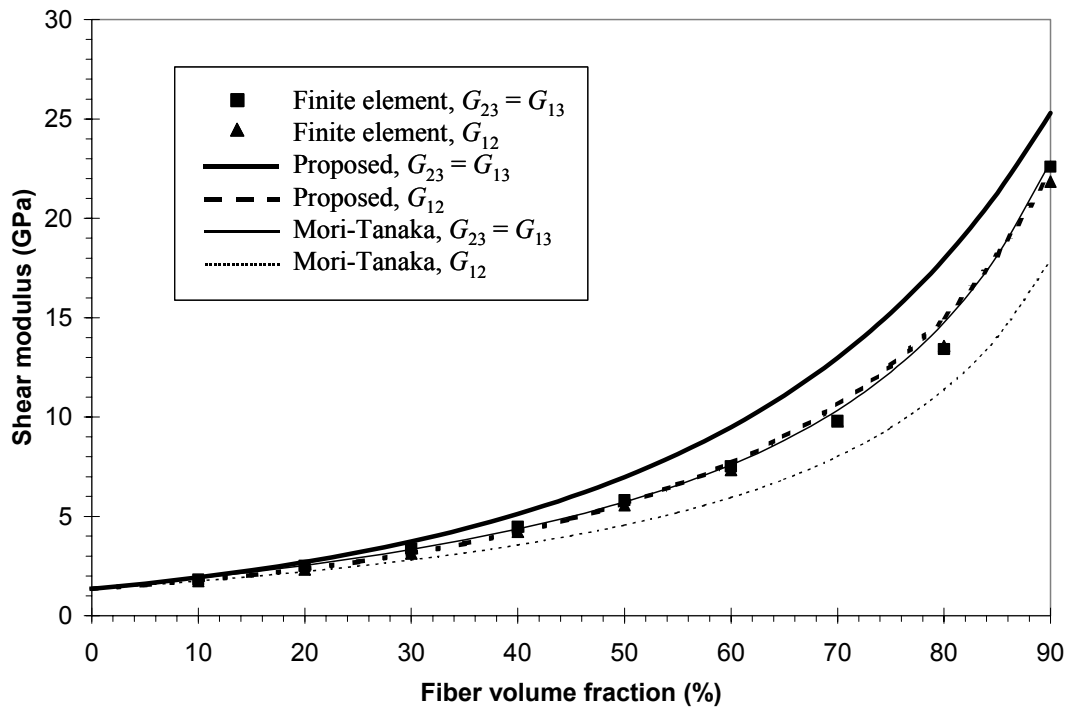Figure 3. *Young's moduli vs. fiber volume fraction for graphite/PVDF composite*
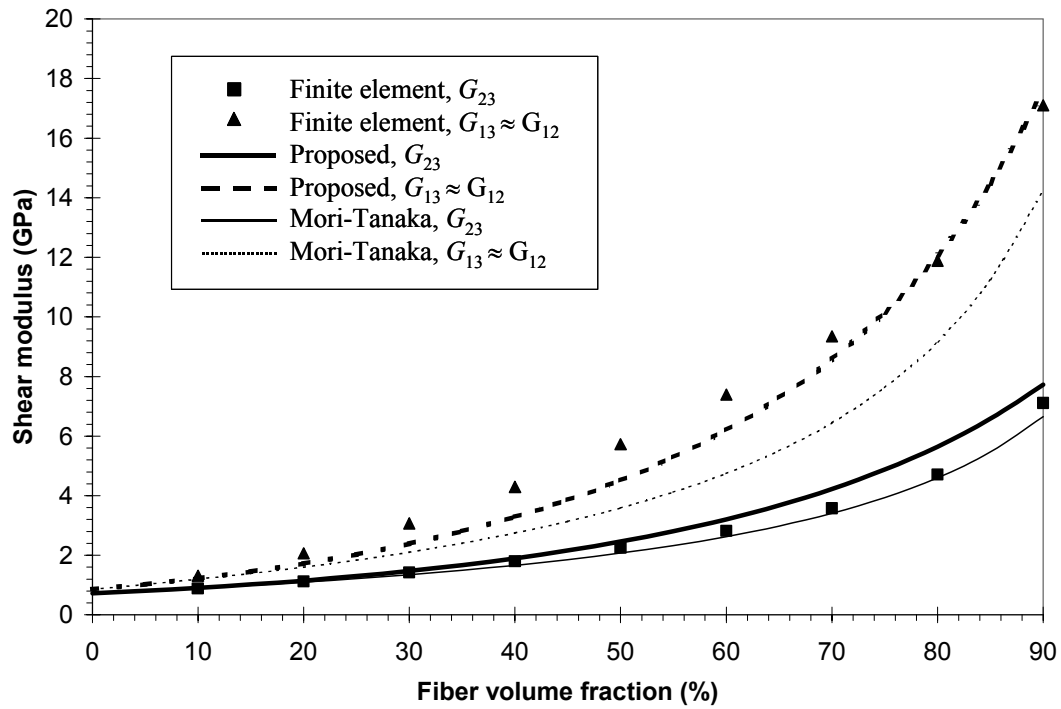
Figure 4. *Shear moduli vs. fiber volume fraction for graphite/PVDF composite*
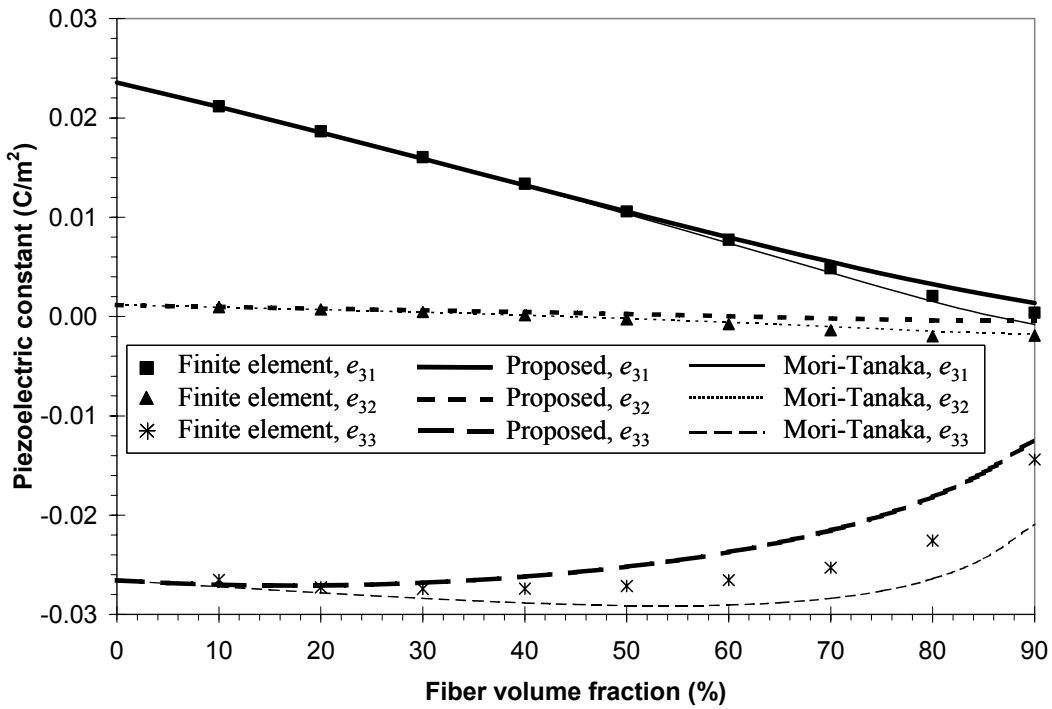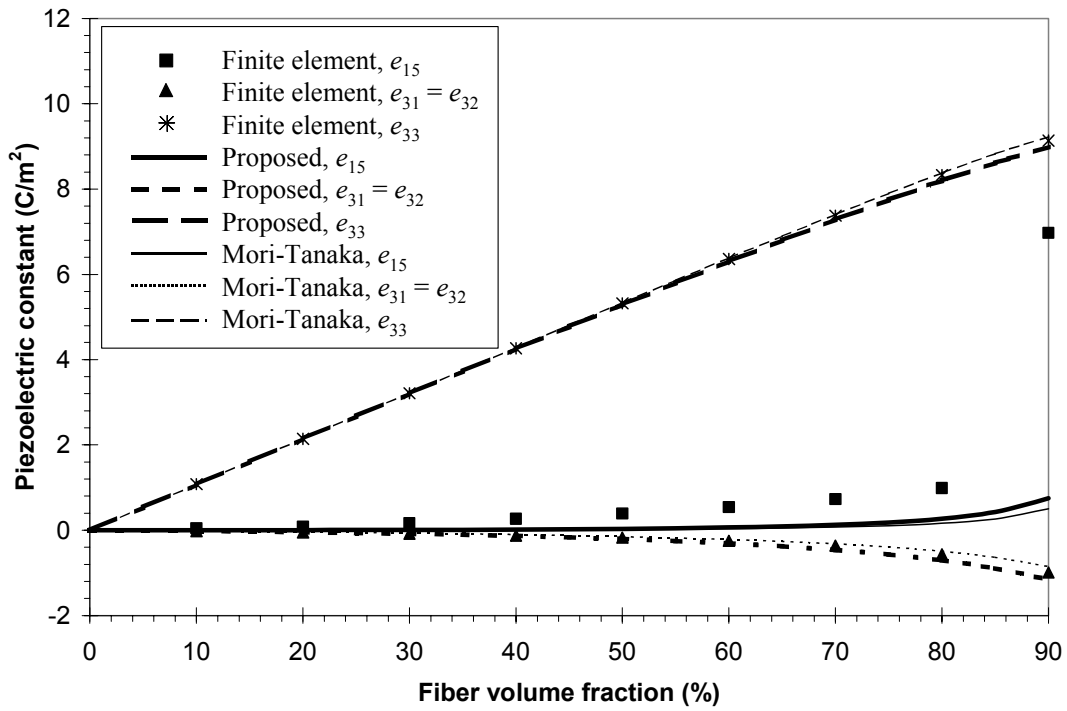
Figure 5. *Piezoelectric constants vs. fiber volume fraction for graphite/PVDF composite*
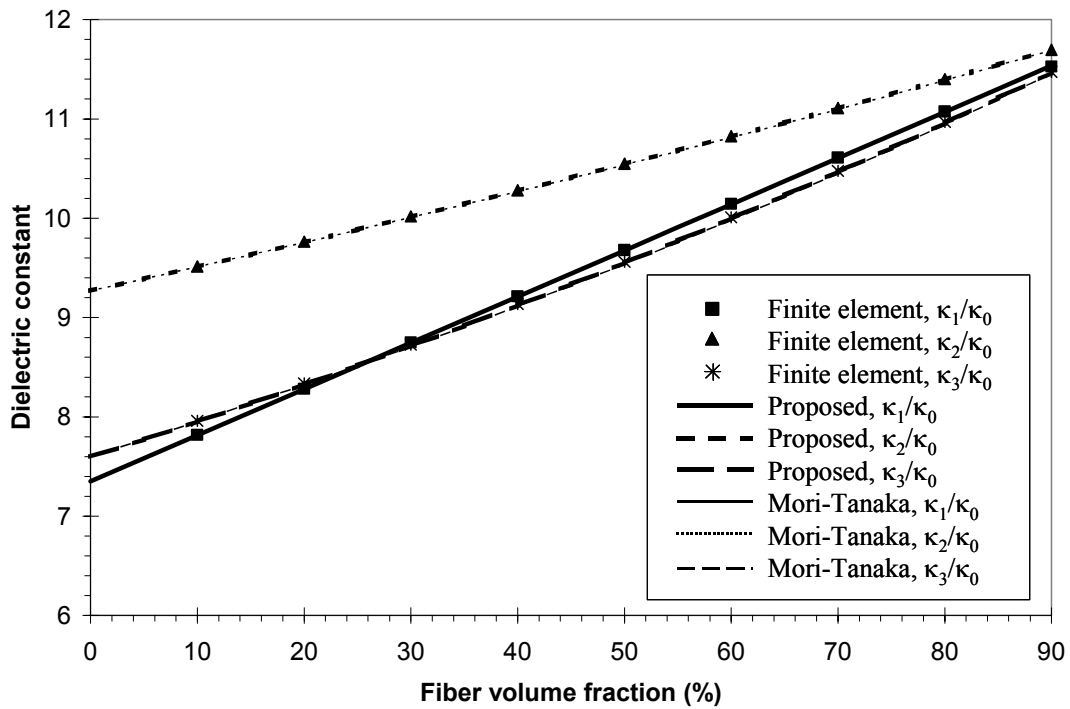
Figure 6. *Dielectric constants vs. fiber volume fraction for graphite/PVDF composite*
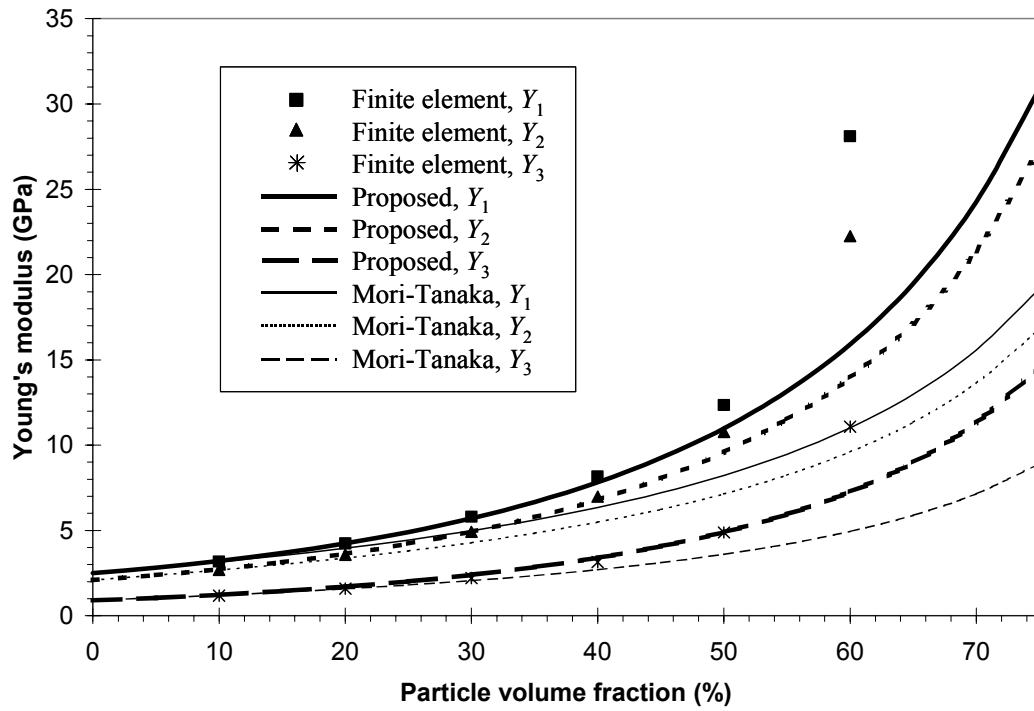
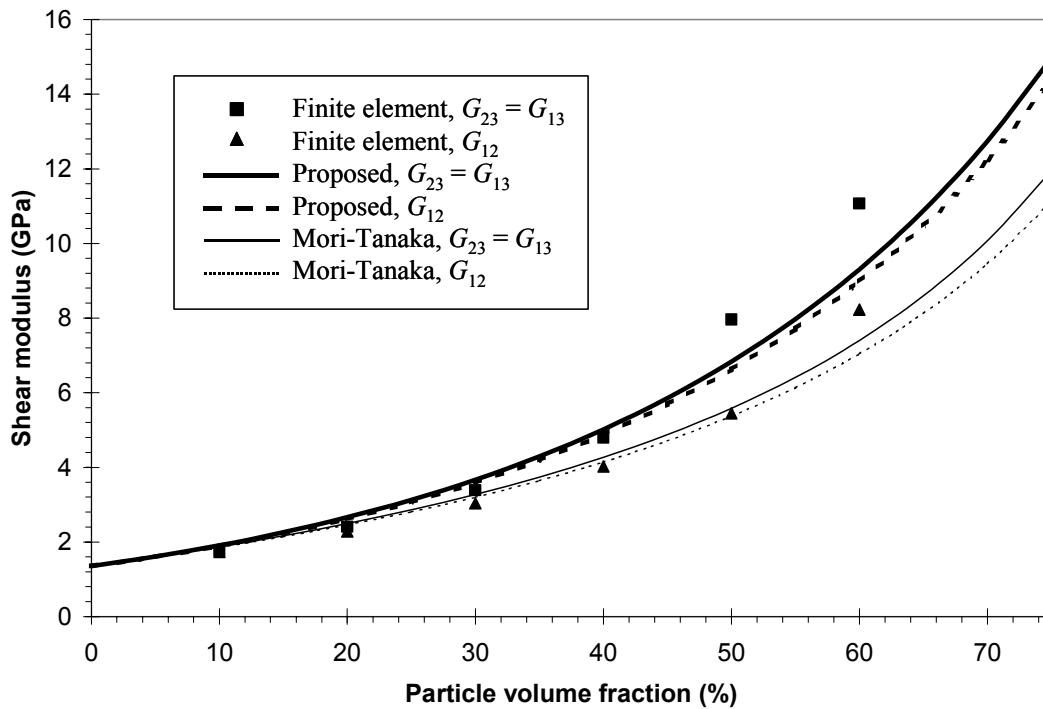Figure 7. *Young's moduli vs. particle volume fraction for SiC/PVDF composite*
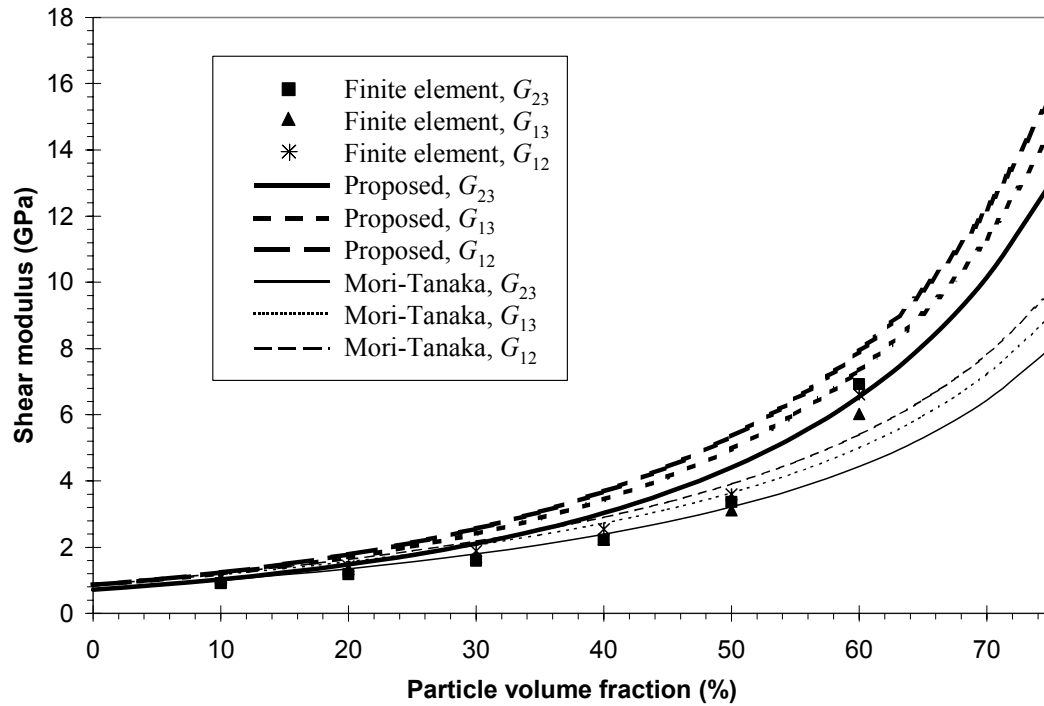
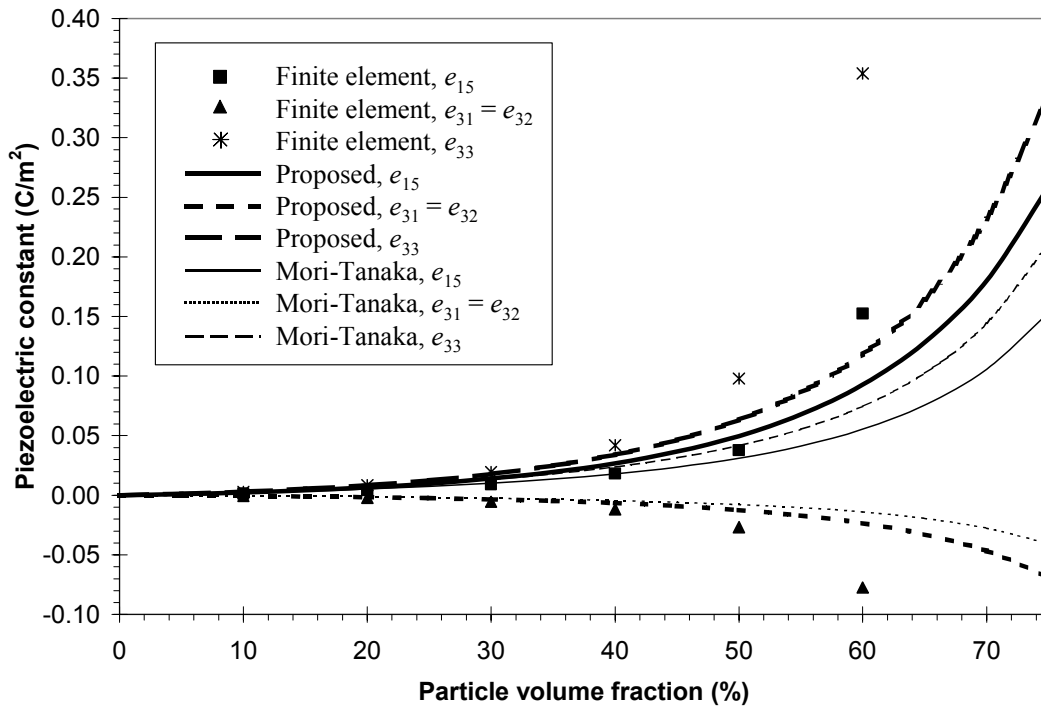Figure 8. *Shear moduli vs. particle volume fraction for SiC/PVDF composite*

23
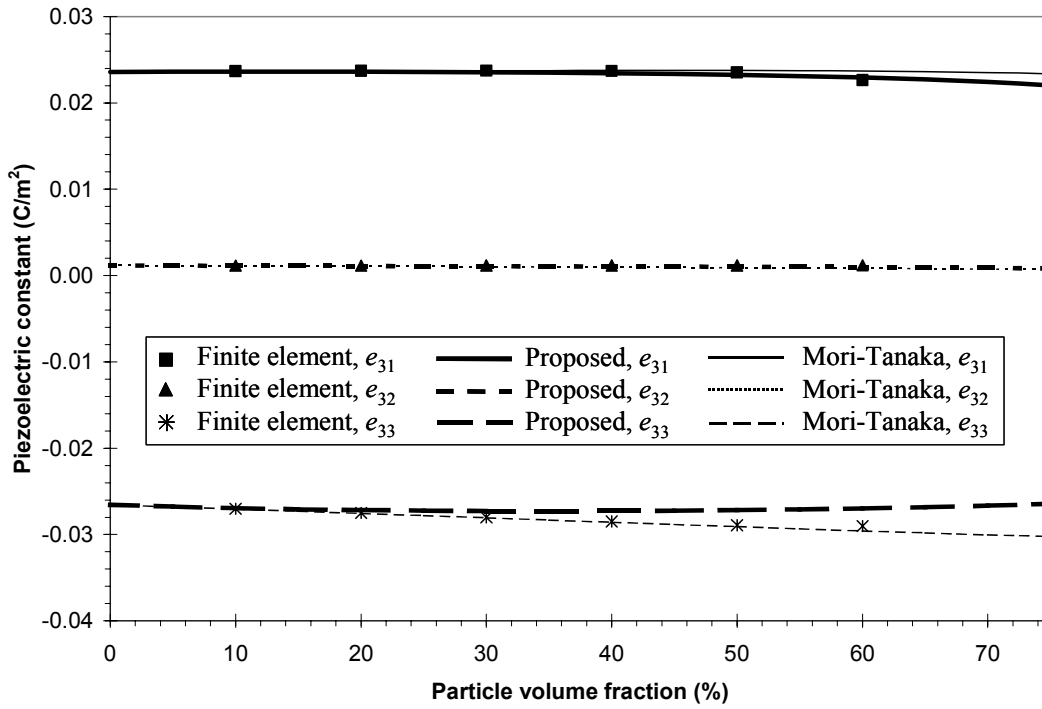
Figure 9. *Piezoelectric constants vs. particle volume fraction for SiC/PVDF composite*
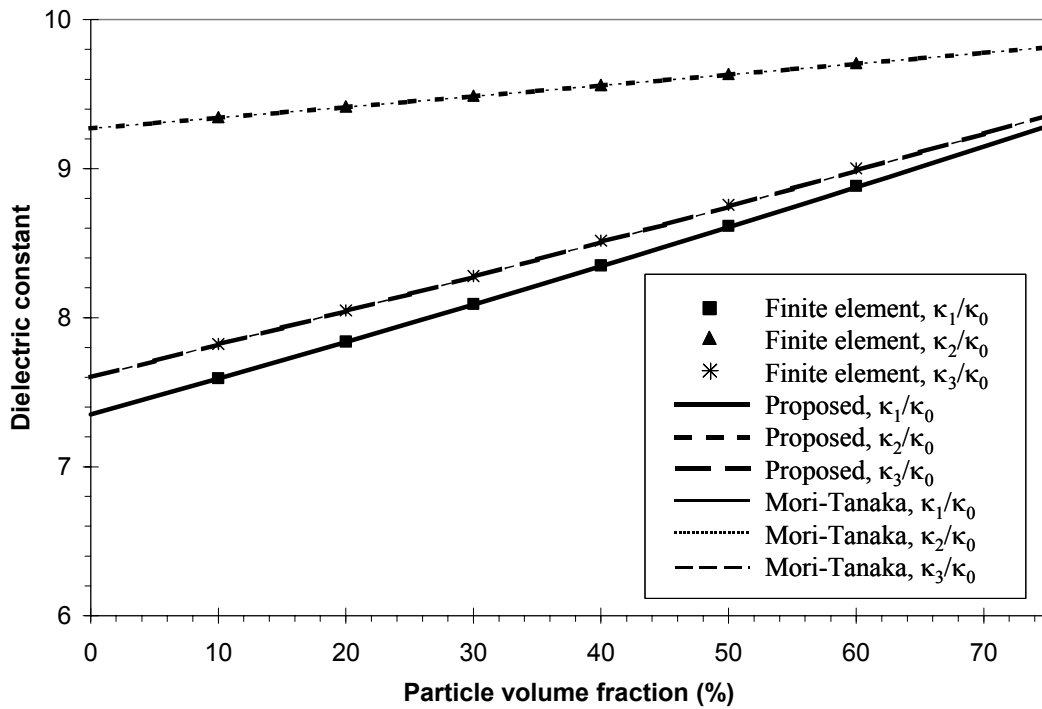
Figure 10. *Dielectric constants vs. particle volume fraction for SiC/PVDF composite*
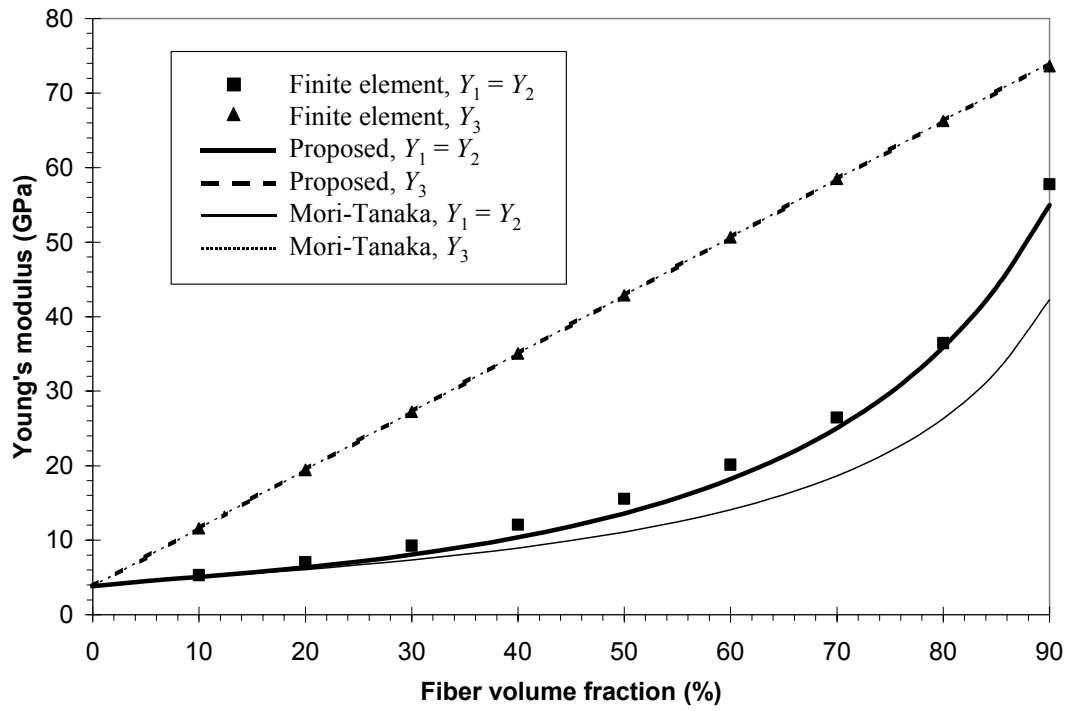
Figure 11. *Young's moduli vs. fiber volume fraction for PZT-7A/LaRC-SI composite*

Figure 12. *Shear moduli vs. fiber volume fraction for PZT-7A/LaRC-SI composite*

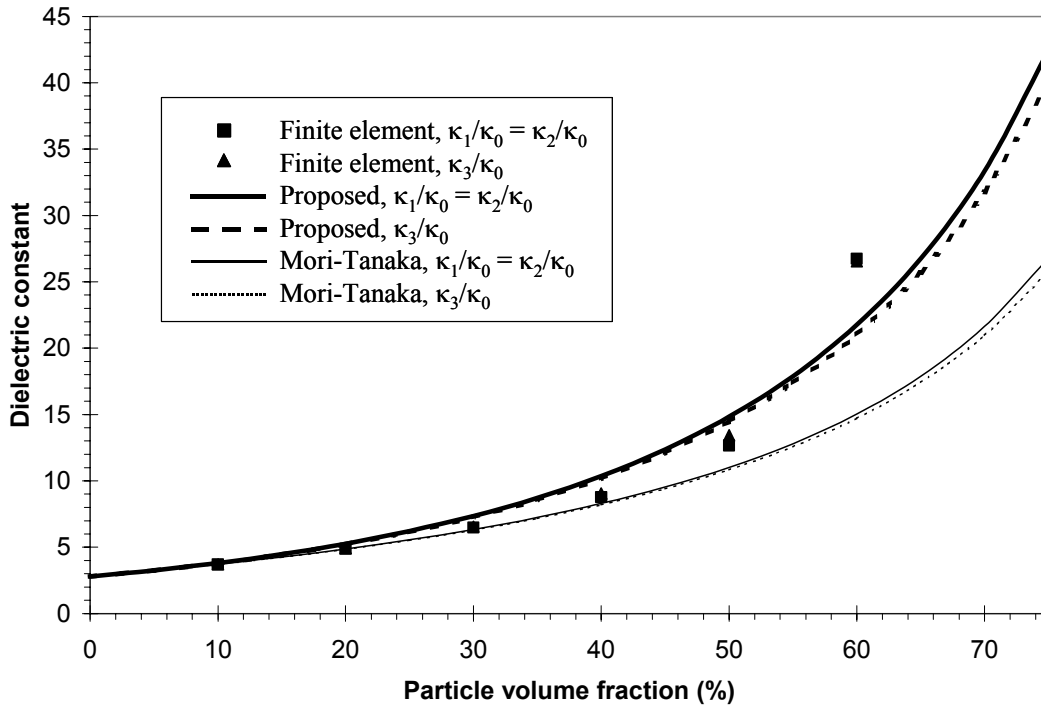Figure 13. *Piezoelectric constants vs. fiber volume fraction for PZT-7A/LaRC-SI composite*
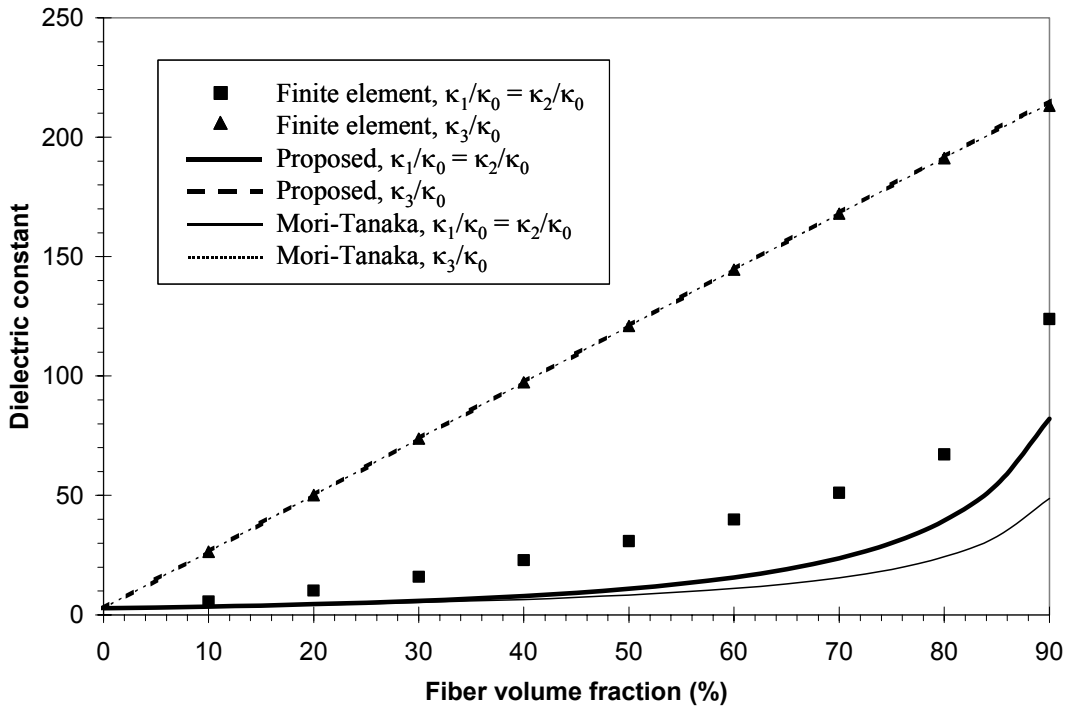
Figure 14. *Dielectric constants vs. fiber volume fraction for PZT-7A/LaRC-SI composite*
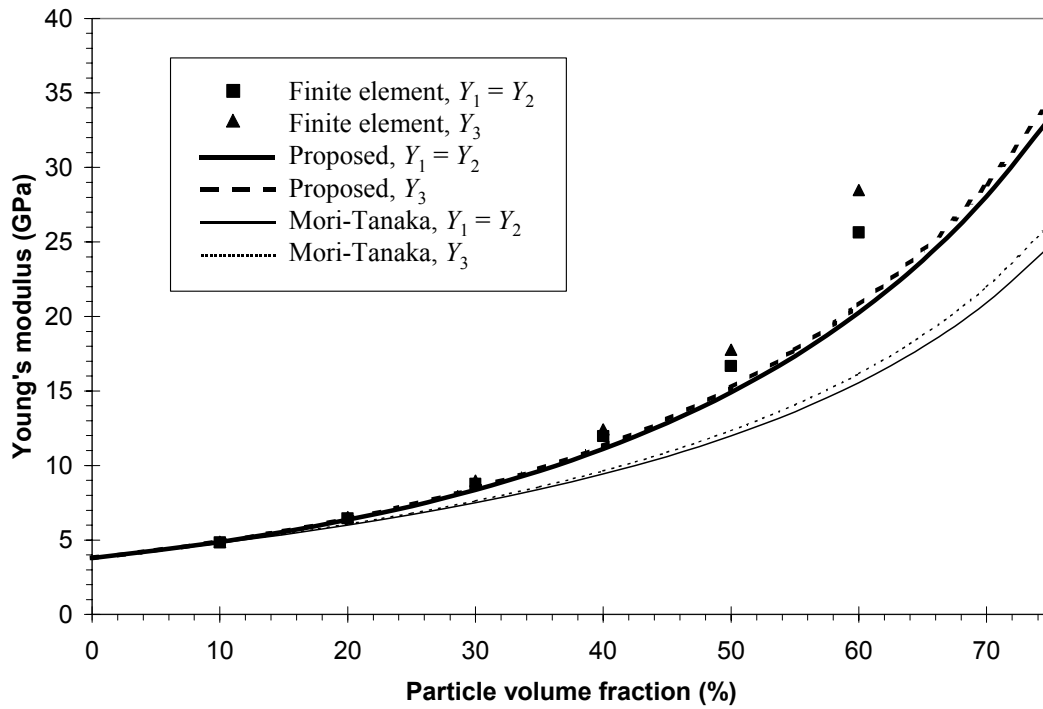
Figure 15. *Young's moduli vs. particle volume fraction for PZT-7A/LaRC-SI composite*

Figure 16. *Shear moduli vs. particle volume fraction for PZT-7A/LaRC-SI composite*

Figure 17. *Piezoelectric constants vs. particle volume fraction for PZT-7A/LaRC-SI composite*

Figure 18. *Dielectric constants vs. particle volume fraction for PZT-7A/LaRC-SI composite*

REPORT DOCUMENTATION PAGE

1. REPORT DATE *(DD-MM-YYYY)*	2. REPORT TYPE	3. DATES COVERED *(From - To)*

4. TITLE AND SUBTITLE	5a. CONTRACT NUMBER
	5b. GRANT NUMBER
	5c. PROGRAM ELEMENT NUMBER

6. AUTHOR(S)	5d. PROJECT NUMBER
	5e. TASK NUMBER
	5f. WORK UNIT NUMBER

7. PERFORMING ORGANIZATION NAME(S) AND ADDRESS(ES)	8. PERFORMING ORGANIZATION REPORT NUMBER

9. SPONSORING/MONITORING AGENCY NAME(S) AND ADDRESS(ES)	10. SPONSORING/MONITOR'S ACRONYM(S)
	11. SPONSORING/MONITORING REPORT NUMBER

12. DISTRIBUTION/AVAILABILITY STATEMENT

13. SUPPLEMENTARY NOTES

14. ABSTRACT

15. SUBJECT TERMS

16. SECURITY CLASSIFICATION OF:			17. LIMITATION OF ABSTRACT	18. NUMBER OF PAGES	19b. NAME OF RESPONSIBLE PERSON
a. REPORT	b. ABSTRACT	c. THIS PAGE			
					19b. TELEPHONE NUMBER *(Include area code)*